

## PDF hosted at the Radboud Repository of the Radboud University Nijmegen

The following full text is a publisher's version.

For additional information about this publication click this link.

<http://hdl.handle.net/2066/72423>

Please be advised that this information was generated on 2017-12-06 and may be subject to change.

## First-principles studies of water adsorption on graphene: The role of the substrate

Tim O. Wehling,<sup>1,a)</sup> Alexander I. Lichtenstein,<sup>1</sup> and Mikhail I. Katsnelson<sup>2</sup>

<sup>1</sup>*I. Institut für Theoretische Physik, Universität Hamburg, Jungiusstraße 9, D-20355 Hamburg, Germany*

<sup>2</sup>*Institute for Molecules and Materials, Radboud University of Nijmegen, Heijendaalseweg 135, 6525 AJ Nijmegen, The Netherlands*

(Received 16 September 2008; accepted 3 November 2008; published online 20 November 2008)

We investigate the electronic properties of graphene upon water adsorption and study the influence of the SiO<sub>2</sub> substrate in this context using density functional calculations. Perfect suspended graphene is rather insensitive to H<sub>2</sub>O adsorbates, as doping requires highly oriented H<sub>2</sub>O clusters. For graphene on a defective SiO<sub>2</sub> substrate, we find a strongly different behavior: H<sub>2</sub>O adsorbates can shift the substrate's impurity bands and change their hybridization with the graphene bands. In this way, H<sub>2</sub>O can lead to doping of graphene for much lower adsorbate concentrations than for free hanged graphene. The effect depends strongly on the microscopic substrate properties. © 2008 American Institute of Physics. [DOI: 10.1063/1.3033202]

Graphene, i.e., a monolayer of graphite, is the first truly two dimensional material<sup>1,2</sup> and a promising candidate for silicon replacement in semiconductor industry<sup>3</sup> or gas sensing applications.<sup>4,5</sup> Since graphene's discovery the water adsorbates have been discussed as impurities leading to doping,<sup>1,4</sup> while changing the electron mobility in graphene only surprisingly little. Up to now, the microscopic mechanism of this doping without significant changes in electron mobility has remained unclear. Density functional theory (DFT) calculations on single water molecule adsorbates on perfect free standing graphene<sup>6</sup> were in line with previous studies on carbon nanotubes (CNTs) (Ref. 7) and found H<sub>2</sub>O physisorption but no H<sub>2</sub>O induced impurity states close to the Fermi level. Therefore, the doping effects found experimentally<sup>1,4</sup> are very likely due to more complicated mechanisms than interactions of graphene with single water molecules. The experiments dealing with the effect of water on graphene were carried out using graphene on top of SiO<sub>2</sub> substrates. In addition, for finite concentrations of H<sub>2</sub>O on graphene H<sub>2</sub>O clusters might form. However, a microscopic theory on the role of the substrate and H<sub>2</sub>O clusters in the H<sub>2</sub>O graphene interplay has been lacking so far. Apart from the topic of doping water is considered important for various other properties of graphene. Water might contribute to bonding of graphene to its substrate<sup>8</sup> and its hydrolysis products could be used to functionalize graphene and create graphene field effect transistors.<sup>9,10</sup>

In this letter we study the substrate and cluster formation effects in the water graphene system by means of DFT. We show that both highly oriented water clusters as well as water adsorbates in combination with a defective SiO<sub>2</sub> substrate can lead to doping of graphene. To this end, we consider model systems (see Fig. 1) for water and ice in different concentrations on free standing graphene as well as for water interacting with defective SiO<sub>2</sub> substrates. By analyzing the involved dipole moments and comparison to electrostatic force microscopy,<sup>11</sup> we show that the SiO<sub>2</sub> substrate is crucial for obtaining doping by H<sub>2</sub>O adsorbates on graphene.

In our DFT calculations, the electronic and structural properties of the graphene-substrate-adsorbate systems are

obtained using generalized gradient approximation (GGA) (Refs. 12 and 13) to the exchange correlation potential. For solving the resulting Kohn–Sham equation we used the Vienna Ab Initio Simulation Package (VASP) (Ref. 14) with the projector augmented wave<sup>15,16</sup> basis sets and 875 eV as plane wave cutoff. The graphene-substrate-adsorbate systems are modeled using supercells containing up to 83 substrate atoms (Si, O, and H), 12 adsorbate atoms, and 32 C atoms. In the total energy calculations and during the structural relaxations the *k*-meshes for sampling of the supercell Brillouin zone were chosen to be as dense as 24 × 24 and 12 × 12 *k*-mesh, respectively, when folded up to the simple graphene unit cell.

First, water adsorption on free standing graphene with different water concentrations is considered. To model a single H<sub>2</sub>O molecule on graphene, 3 × 3 graphene supercells were used. Full relaxation of H<sub>2</sub>O with oxygen [depicted in

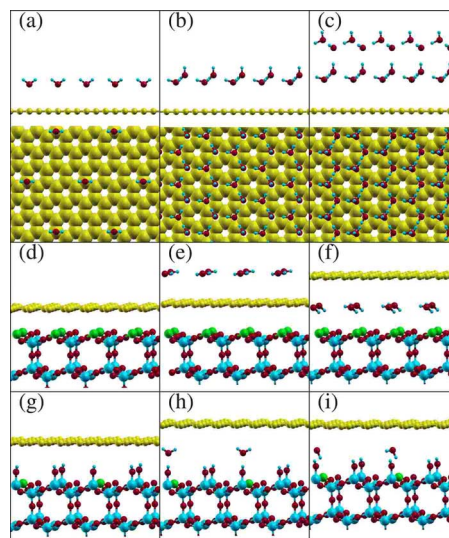


FIG. 1. (Color online) Model systems for water interacting with graphene. [(a)–(c)] Free standing graphene with single water adsorbates (a), a bilayer (b), and a tetralayer (c) of ice Ih. Carbon atoms yellow, oxygen red, and hydrogen small blue balls. [(d)–(i)] Graphene on top of SiO<sub>2</sub> with every second [(d)–(f)] or eighth [(g)–(i)] surface Si atom forming a Q<sub>3</sub><sup>0</sup> defect. Water adsorbates are considered on top of graphene (e) and between the graphene and the substrate (f), (h), and (i). Fully coordinated Si atoms are depicted as big blue balls, Si atoms at Q<sub>3</sub><sup>0</sup> defects in green.

<sup>a)</sup>Electronic mail: twehling@physnet.uni-hamburg.de.

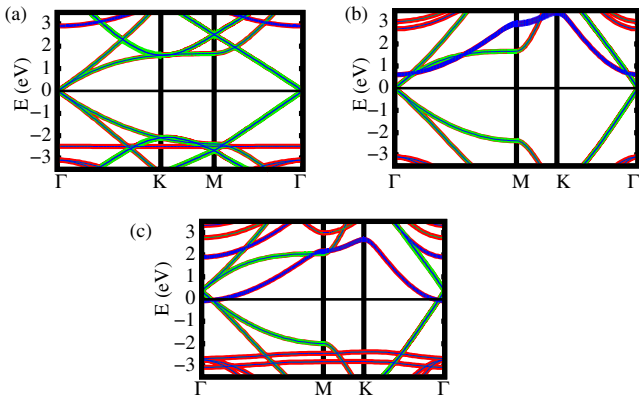


FIG. 2. (Color online) Band structures of supercells with fully relaxed single molecules (a), a bilayer (b), and a tetralayer (c) of water on graphene corresponding to Figs. 1(a)–1(c), respectively, are shown. The graphene  $\pi$  bands are marked in green, the nearly free electron bands in blue. Due to the  $\text{H}_2\text{O}$  dipole moments, graphene's nearly free electron band is shifted with respect to its  $\pi$  bands.

Fig. 1(a)] or hydrogen nearest to the graphene yielded adsorbed configurations with binding energies of 40 and 36 meV and molecule sheet distances of 3.50 and 3.25 Å, respectively. These values are in the same order as those obtained by Leenaerts *et al.*,<sup>6</sup> indicating physisorption of single water molecules on graphene. Analyzing the density of states/band structures for these two adsorption geometries we find qualitative agreement with Refs. 6 and 17: none of these configurations exhibits energy levels due to the adsorbate near the Dirac point, as shown in Fig. 2(a), for the configuration with oxygen closest to graphene. The highest occupied molecular orbital of  $\text{H}_2\text{O}$  is more than 2.4 eV below the Fermi energy and its lowest unoccupied molecular orbital is more than 3 eV above it. The absence of any additional impurity level close to the Dirac point is independent of the  $\text{H}_2\text{O}$  orientation and its lateral position.<sup>18</sup> This shows that single water molecules on perfect free standing graphene sheets do not cause any doping.

The supercell applied here corresponds to an adsorbate concentration of  $n=2 \text{ nm}^{-2}$ , which is well inside the range of concentrations ( $1\text{--}10 \text{ nm}^{-2}$ ) found experimentally in Ref. 11. The lateral dimension  $a=4.5 \text{ Å}$  of the hexagonal ice Ih (0001)-surface unit cell corresponds to a concentration of  $5.7 \text{ H}_2\text{O nm}^{-2}$  per layer. Thus, increasing the  $\text{H}_2\text{O}$  concentration significantly above the  $n=2 \text{ nm}^{-2}$  from above leads to water clusters or icelike structures, rather than isolated molecules.

To gain insight into doping of graphene by water clusters and ice overlayers we studied fully relaxed<sup>19</sup> bilayers and four layers of ice Ih adsorbed on graphene. These overlayer structures have been proposed as basis of ice growth on various hexagonal metal surfaces<sup>20,21</sup> and can be modeled as  $(\sqrt{3} \times \sqrt{3})R30^\circ$  overlayer on the simple graphene unit cell. The lattice mismatch in this configuration is 0.23 Å—on the same order as found for water overlayers on Ni(111) (Ref. 20)—and therefore a reasonable starting point for studying ice on graphene.

The supercell band structures [Figs. 2(b) and 2(c)] show that the electric field by proton-ordered ice on top of graphene changes the energy of graphene's nearly free electron bands. In contrast to pristine graphene, where these bands start at 3 eV above the Dirac point or in the case of single  $\text{H}_2\text{O}$  adsorbates on graphene [Fig. 2(a)], their bottom

is at 0.6 eV above and 0.1 eV below the Dirac point for a bi- and a tetralayer of ice Ih on top of graphene. This shift is due to electrostatic fields induced by the  $\text{H}_2\text{O}$  dipole moments and results in hole doping for the tetralayer of ice on graphene.

The water adlayers cause a change in contact potential  $\delta\phi$ , which can be estimated using the  $\text{H}_2\text{O}$  dipole moment  $p=6.2 \times 10^{-30} \text{ C m}$  and the relaxed structures to be  $\delta\phi=1.4$  and 5.4 V for a water bi- and tetralayer, respectively. While only the latter structure causes doping, the corresponding change in contact potential exceeds the experimental value  $\delta\phi_{\text{exp}}=1.3 \text{ V}$  in Ref. 11 by more than a factor of 4. However, water strongly diluted in  $\text{N}_2$  has been found to cause hole doping in graphene on  $\text{SiO}_2$ .<sup>4</sup> Given these two experiments, doping due to multiple fully oriented ice overlayers as in Fig. 2 is likely not the most important interaction mechanism for water and graphene.

We now turn to studying the effect of the  $\text{SiO}_2$  substrate in the water-graphene interplay. The  $\text{SiO}_2$  surfaces used in the experiments<sup>4,11</sup> are amorphous and challenging to model from first principles. To obtain qualitative insight to the most important physical mechanisms, it is, however, a reasonable starting point to consider crystalline  $\text{SiO}_2$  in the  $\beta$ -cristobalite form as a substrate.<sup>22</sup>

The (111) surface of this modification can be used to create the most likely defects on  $\text{SiO}_2$  amorphous surfaces. These are the so called  $Q_3^0$  and  $Q_4^1$  defects<sup>23</sup> having one under coordinated silicon and oxygen atom, respectively. Furthermore, the unit cell of this surface is nearly commensurate with the graphene lattice. The lattice constant  $a_{\text{SiO}_2}=7.13 \text{ Å}$  (Ref. 24) results in a surface unit cell  $a_{\text{SiO}_2}/\sqrt{2}=5.04 \text{ Å}$ , which is 4% larger than twice the lattice constant  $2a_0=4.93 \text{ Å}$  of graphene. As the  $\text{SiO}_4$  tetrahedra in  $\text{SiO}_2$  are known to adjust to external strain easily, we model graphene on  $\text{SiO}_2$  by  $2 \times 2$  or  $4 \times 4$  graphene supercells with lateral dimension  $2a_0$  or  $4a_0$ . As substrate we put 4% laterally strained and hydrogen passivated  $\beta$ -cristobalite with six Si atoms per surface unit cell in vertical direction. We then created the defects by removing H passivation atoms, added the  $\text{H}_2\text{O}$  adsorbates, and relaxed until all forces were less than  $0.08 \text{ eV Å}^{-1}$ . In this way, we consider passivated and defective  $\text{SiO}_2$  surfaces—the latter containing either undercoordinated silicon or oxygen atoms—as substrate for graphene. The effect of water exposure is simulated by putting water molecules on top of graphene as well as between the graphene and the substrate.

Graphene on top of fully passivated  $\text{SiO}_2$  means two inert systems are in contact with each other. Consequently, there are no bands in addition to graphene's Dirac bands at the Fermi level and no doping occurs. (The band structure is not shown here for brevity.) This changes strongly for graphene on defective  $\text{SiO}_2$ . As a model system, we study  $Q_3^0$  defects in  $\beta$ -cristobalite (111) surfaces. Depending on the supercell size,  $2 \times 2$  and  $4 \times 4$ , in these periodic structures every second and eighth surface Si atom is under coordinated, respectively, and forms a  $Q_3^0$  defect [see Figs. 1(d)–1(i)].

These defects lead to additional states in the vicinity ( $\pm 1 \text{ eV}$ ) around the Fermi level [see Figs. 3(a) and 3(d)].

The avoided crossing in Fig. 3(a) indicates a significant hybridization of the defect and the graphene bands and demonstrates the impurity state's importance for conduction elec-

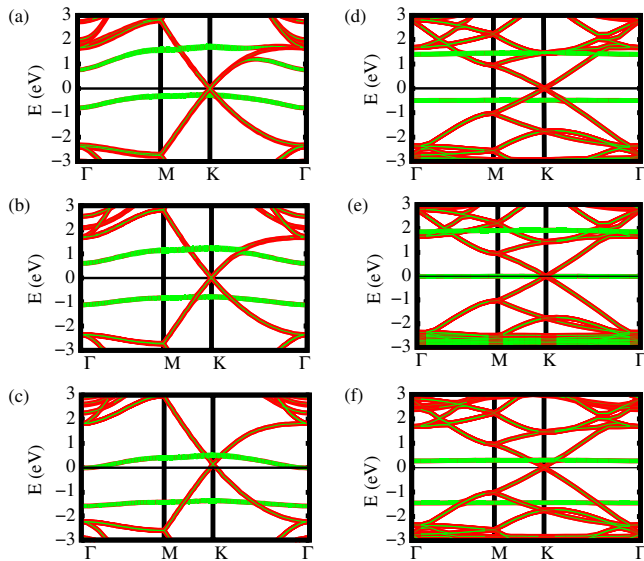


FIG. 3. (Color online) Band structures for graphene on defective  $\text{SiO}_2$  substrates. [(a)–(c)]  $2 \times 2$  and [(d)–(f)]  $4 \times 4$  graphene supercells with every second [(a)–(c)] or eighth [(d)–(f)] surface Si atom forming a  $Q_3^0$  defect. The corresponding geometries are shown in Figs. 1(d)–1(i), respectively. Spin up and down bands are shown at the same time. Contributions at the defect site are marked as green fat bands. (a) and (d) Without water adsorbates. (b) With water on top of graphene. (c), (e), and (f) With water between the graphene and the substrate. (c) and (f)  $\text{H}_2\text{O}$  dipole moment pointing tilted downward. (e)  $\text{H}_2\text{O}$  dipole moment pointing upward.

tron scattering in graphene. In the pure  $\text{SiO}_2$  graphene model systems [Figs. 3(a) and 3(d)], the impurity bands do not cross the Fermi level. This situation can be changed by water adsorbates, which may sit either in between the graphene and the substrate [Figs. 3(c), 3(e), and 3(f)] or on top of graphene [Fig. 3(b)]. In all cases, the electrostatic dipole moment of the water adsorbates comes along with strong local electrostatic fields, which allow to shift the impurity bands significantly with respect to the graphene bands. As Fig. 3 demonstrates, this shift strongly depends on the place of adsorption and the orientation of the water molecules, leading either to hole doping [Figs. 3(c) and 3(f)] or electron doping [Fig. 3(e)].

This strong effect of water is very general and not limited to the examples shown in Fig. 3. Similar effects of water can be found for graphene on the (0001) plane of  $\alpha$ -quartz or  $\beta$ -cristobalite with  $Q_4^1$  defects. Although the interaction mechanisms of water,  $\text{SiO}_2$ , and graphene presented here are not exhaustive, the comparison of water adsorption on perfect free standing graphene to water adsorption on graphene lying on a (defective)  $\text{SiO}_2$  substrate allows the following conclusions: perfect free standing graphene may have water adsorbates on top but its electronic transport properties are insensitive against perturbations by the water adsorbates. Single molecules will not create any impurity states close to the Dirac point. For obtaining doping effects, one needs highly ordered  $\text{H}_2\text{O}$  cluster or ice structures.

The substrate changes the situation completely. The dipole moments of  $\text{H}_2\text{O}$  adsorbates cause local electrostatic fields that can shift the substrate's defect states with respect to the graphene electrons and cause doping. The hybridization of substrate defect states with the graphene bands can be reduced by  $\text{H}_2\text{O}$  in between the graphene and the substrate, leading to less scattering of graphene electrons at defects in the substrate. On the other hand, impurity bands can be

shifted toward the Fermi level by  $\text{H}_2\text{O}$  adsorbates, leading to increased electron scattering. So, for graphene on a substrate,  $\text{H}_2\text{O}$  much more likely affects the electronic properties than for free standing graphene. The effect of water strongly depends on properties of the substrate such as the amount and type of defects.

This finding might explain experiments on CNTs:<sup>25</sup> CNTs on  $\text{SiO}_2$  substrates are much more sensitive to water in their environment than suspended CNTs or CNTs separated from the  $\text{SiO}_2$  substrate by poly(methylmethacrylate) (PMMA) coating. In experiments similar to those in Refs. 3 and 26 these effects can be checked for graphene. Some molecules like  $\text{NO}_2$  lead to acceptor states even without a substrate<sup>5</sup> while doping effects due to other molecules like  $\text{H}_2\text{O}$  strongly depend on the substrate. This can open the possibility of selective graphene gas sensors.

The authors are thankful to Andre Geim and Kostya Novoselov for the inspiring discussions. This work was supported by SFB 668 (Germany) and FOM (The Netherlands). Computation time at HLRN is acknowledged.

- <sup>1</sup>K. S. Novoselov, A. K. Geim, S. V. Morozov, D. Jiang, Y. Zhang, S. V. Dubonos, I. V. Grigorieva, and A. A. Firsov, *Science* **306**, 666 (2004).
- <sup>2</sup>K. S. Novoselov, D. Jiang, F. Schedin, T. J. Booth, V. V. Khotkevich, S. V. Morozov, and A. K. Geim, *Proc. Natl. Acad. Sci. U.S.A.* **102**, 10451 (2005).
- <sup>3</sup>S. V. Morozov, K. S. Novoselov, M. I. Katsnelson, F. Schedin, D. C. Elias, J. A. Jaszczak, and A. K. Geim, *Phys. Rev. Lett.* **100**, 016602 (2008).
- <sup>4</sup>F. Schedin, A. K. Geim, S. V. Morozov, E. W. Hill, P. Blake, M. I. Katsnelson, and K. S. Novoselov, *Nature Mater.* **6**, 652 (2007).
- <sup>5</sup>T. O. Wehling, K. S. Novoselov, S. V. Morozov, E. E. Vdovin, M. I. Katsnelson, A. K. Geim, and A. I. Lichtenstein, *Nano Lett.* **8**, 173 (2008).
- <sup>6</sup>O. Leenaerts, B. Partoens, and F. M. Peeters, *Phys. Rev. B* **77**, 125416 (2008).
- <sup>7</sup>J. Zhao, A. Buldum, J. Han, and J. P. Lu, *Nanotechnology* **13**, 195 (2002).
- <sup>8</sup>J. Sabio, C. Seoáñez, S. Fratini, F. Guinea, A. H. C. Neto, and F. Sols, *Phys. Rev. B* **77**, 195409 (2008).
- <sup>9</sup>T. J. Echtermeyer, M. C. Lemme, M. Baus, B. N. Szafrank, A. K. Geim, and H. Kurz, "A graphene-based electrochemical switch," arXiv:0712.2026v1.
- <sup>10</sup>J. P. Robinson, H. Schomerus, L. Oroszlany, and V. I. Fal'ko, *Phys. Rev. Lett.* **101**, 196803 (2008).
- <sup>11</sup>J. Moser, A. Verdager, D. Jimenez, A. Barreiro, and A. Bachtold, *Appl. Phys. Lett.* **92**, 123507 (2008).
- <sup>12</sup>J. P. Perdew, J. A. Chevary, S. H. Vosko, K. A. Jackson, M. R. Pederson, D. J. Singh, and C. Fiolhais, *Phys. Rev. B* **46**, 6671 (1992).
- <sup>13</sup>J. P. Perdew, K. Burke, and M. Ernzerhof, *Phys. Rev. Lett.* **77**, 3865 (1996).
- <sup>14</sup>G. Kresse and J. Hafner, *J. Phys.: Condens. Matter* **6**, 8245 (1994).
- <sup>15</sup>P. E. Blöchl, *Phys. Rev. B* **50**, 17953 (1994).
- <sup>16</sup>G. Kresse and D. Joubert, *Phys. Rev. B* **59**, 1758 (1999).
- <sup>17</sup>R. M. Ribeiro, N. M. R. Peres, J. Coutinho, and P. R. Bridson, *Phys. Rev. B* **78**, 075442 (2008).
- <sup>18</sup>At 3 Å or higher above the graphene sheet the potential energy landscape is very flat. The  $\text{H}_2\text{O}$  adsorption energies change by less than 5 meV with lateral position (Ref. 6).
- <sup>19</sup>Starting from overlayers according to the "Bernal–Fowler–Pauling" rules (see Refs. 20 and 27) our relaxations yield the first  $\text{H}_2\text{O}$  layer at 3.8 and 4.0 Å above the graphene sheet for adsorbed bi- and tetralayers, respectively, with oxygen closest to graphene.
- <sup>20</sup>T. Lankau, Habilitation Thesis, University of Hamburg, 2004.
- <sup>21</sup>S. Meng, E. Kaxiras, and Z. Zhang, *J. Chem. Phys.* **127**, 244710 (2007).
- <sup>22</sup>P. Carrier, L. J. Lewis, and M. W. C. Dharma-wardana, *Phys. Rev. B* **64**, 195330 (2001).
- <sup>23</sup>M. Wilson and T. R. Walsh, *J. Chem. Phys.* **113**, 9180 (2000).
- <sup>24</sup>A. Wright and A. Leadbetter, *Philos. Mag.* **31**, 1391 (1975).
- <sup>25</sup>W. Kim, A. Javey, O. Vermesh, Q. Wang, Y. Li, and H. Dai, *Nano Lett.* **3**, 193 (2003).
- <sup>26</sup>X. Du, I. Skachko, A. Barker, and E. Y. Andrei, *Nat. Nanotechnol.* **3**, 491 (2008).
- <sup>27</sup>P. A. Thiel and T. E. Madey, *Surf. Sci. Rep.* **7**, 211 (1987).